



How do spatial scale and seasonal factors affect thermal-based water status estimation and precision irrigation decisions in vineyards?

Idan Bahat^{1,2} · Yishai Netzer^{3,4} · José M. Grünzweig² · Amos Naor⁵ · Victor Alchanatis¹ · Alon Ben-Gal⁶ · Ohali'av Keisar¹ · Guy Lidor¹ · Yafit Cohen¹

Accepted: 31 January 2024
© The Author(s) 2024

Abstract

The crop water stress index (CWSI) is widely used for assessing water status in vineyards, but its accuracy can be compromised by various factors. Despite its known limitations, the question remains whether it is inferior to the current practice of direct measurements of Ψ_{stem} of a few representative vines. This study aimed to address three key knowledge gaps: (1) determining whether Ψ_{stem} (measured in few vines) or CWSI (providing greater spatial representation) better represents vineyard water status; (2) identifying the optimal scale for using CWSI for precision irrigation; and (3) understanding the seasonal impact on the CWSI- Ψ_{stem} relationship and establishing a reliable Ψ_{stem} prediction model based on CWSI and meteorological parameters. The analysis, conducted at five spatial scales in a single vineyard from 2017 to 2020, demonstrated that the performance of the CWSI- Ψ_{stem} model improved with increasing scale and when meteorological variables were integrated. This integration helped mitigate apparent seasonal effects on the CWSI- Ψ_{stem} relationship. R^2 were 0.36 and 0.57 at the vine and the vineyard scales, respectively. These values rose to 0.51 and 0.85, respectively, with the incorporation of meteorological variables. Additionally, a CWSI-based model, enhanced by meteorological variables, outperformed current water status monitoring at both vineyard (2.5 ha) and management cell (MC) scales (0.09 ha). Despite reduced accuracy at smaller scales, water status evaluation at the management cell scale produced significantly lower Ψ_{stem} errors compared to whole vineyard evaluation. This is anticipated to enable more effective irrigation decision-making for small-scale management zones in vineyards implementing precision irrigation.

Keywords Crop water stress index (CWSI) · Stem water potential · Modeling · Thermal imagery · Precision viticulture

Introduction

Accurate control of vine water status during the growing season is required to promote fruit quality in red wine production (Van Leeuwen et al., 2009). Stem water potential (Ψ_{stem}) is a sensitive indicator for vine water status (Choné et al., 2001) and should be frequently and

Extended author information available on the last page of the article

accurately monitored when used to drive vineyard irrigation management (Acevedo-Opazo et al., 2010; Netzer et al., 2019; Van Leeuwen et al., 2009). At the vineyard scale, Ψ_{stem} assessment requires laborious and time-consuming measurements. In earlier studies and in some more recent ones, leaf water potential (Ψ_{leaf}) stood out as the primary approach for assessing plant water status. However, in recent years, it has been demonstrated that Ψ_{stem} is more precise, albeit with the caveat of necessitating preparatory steps that prolong the measurement duration (Choné et al., 2001; Naor, 1998; Santesteban et al., 2019). In current water status monitoring practice, Ψ_{stem} is measured only on a few representative vines. As this method suffers from spatial under-representation, it is prone to major errors in assessing water status when scaled up to an entire vineyard. Aerial remote sensing has been widely utilized to illustrate spatial variations in various crop conditions, including crop water content (e.g. Ndlovu et al., 2021). Nevertheless, reports in the literature suggest limited effectiveness in remotely estimating Ψ_{stem} or Ψ_{leaf} using remote sensing in the visible and the near-infrared (VIS–NIR) regions. This limitation is attributed to the fact that these spectral regions predominantly convey the physical status of water potential within plant tissues (Cohen & Alchanatis, 2018). The alternate electromagnetic spectrum sensitive to plant water status is the far or thermal infrared. A significant outcome of stomatal closure under water stress conditions is the reduction in energy dissipation, leading to an increase in leaf temperature (Jones, 1999). Subsequently, aerial thermal imaging served as an alternative method for assessing the spatial variability of water status (e.g. Matese et al., 2018; Santesteban et al., 2017) and for irrigation scheduling at the vineyard scale (Bellvert et al., 2016a; Matese & Di Gennaro, 2018; Santesteban et al., 2017).

The crop water stress index (CWSI), a relative measure of plant transpiration rate, is the most widely used thermal-based index for assessing plant water status (Idso et al., 1981). Previous studies have shown water status assessment inaccuracies using CWSI derived from thermal imaging. Errors can be grouped into four major types: (1) Errors arising from the varying influence of physiological conditions on the relationships between CWSI and water status. Möller et al. (2007) reported CWSI- Ψ_{stem} correlations with a lower coefficient of determination at the end of the season because of partial leaf senescence within the vineyard canopy. Bellvert et al. (2016a) reported little response of leaf water potential (Ψ_{leaf}) to changes in CWSI in early phenological stages and also for different grapevine varieties. An improvement in the CWSI- Ψ_{stem} relationship was shown for specific phenological and varietal relationships compared to general relationships (Bellvert et al., 2014a). These findings were supported by trends observed in vineyards in Israel, where CWSI- Ψ_{stem} relations at early phenological stages of the season were not well-correlated (Fig. 7). (2) Errors arising from the varying influence of atmospheric conditions on the relationships between CWSI and water status. Sepúlveda-Reyes et al. (2016) obtained the best relationship of CWSI- Ψ_{stem} on days with maximum seasonal atmospheric demand. Air temperature (T_a) is considered a major error contributor as $\pm 1^\circ\text{C}$ error in T_a led to 28–82% disparity for CWSI calculation in orange trees (Gonzalez-Dugo & Zarco-Tejada 2022) (3) inconsistency arising from the selection of the method employed for computing CWSI. There are several methods to estimate CWSI, either analytical, empirical (Maes & Steppe, 2012), or statistical approaches (e.g. Alchanatis et al., 2010; Rud et al., 2014) using different procedures for the calculation of the parameters representing the range of possible high (T_{dry}) and low (T_{wet}) temperatures used to normalize measured canopy temperature. Comparisons between different approaches illuminated major disparities (Agam et al., 2013a, 2013b; Cohen et al., 2015). (4) Errors arising from the characteristics of the aerial thermal images and the conditions in which they were acquired. Bellvert et al.

(2016b) demonstrated in vineyards that the best results were obtained at the smallest, 0.3 m pixel size, due to improvement in extraction of pure canopy pixels. The process of mosaicking (stitching single images to capture the total area of interest) could also cause a decrease in image quality due to various factors such as registration errors, geometric distortion, and radiometric differences between images (Ghosh & Kaabouch, 2016). Time of image acquisition was found to be best at solar noon (12:30) compared to morning (Alchanatis et al., 2010; Bellvert et al., 2014b; Fuentes et al., 2012).

Although CWSI- Ψ_{stem} model accuracy might be compromised by the above-mentioned error sources, the question remains whether it is inferior to existing water status monitoring alternatives based on direct measurements of Ψ_{stem} of a few representative vines. Comparison between the two approaches can only be conducted using extensive Ψ_{stem} measurements on multiple vines representing the entire vineyard's spatial variability. To the best of our knowledge, such a comparison has not yet been conducted. As described above, relationships between CWSI and Ψ_{stem} can differ as a function of phenological growth stage and change under different physiological and meteorological conditions. The extent to which these relationships change while moving from single-vine to management zone (MZ) and to the vineyard scale has yet to be investigated. The fundamental hypothesis guiding this study posited that, under a fixed image resolution, a smaller area of interest—like a single vine with fewer pixels—would correspond to decreased efficacy in CWSI's ability to estimate water status, consequently leading to heightened errors. Examining a broader area of interest, such as a vineyard or a management zone (MZ), enhances the CWSI's capacity to estimate water status, as it involves a larger number of pixels for its representation. Most prior thermal-based water assessment studies were focused on the vineyard scale (Table 1). To apply precision irrigation, large vineyards are delineated into smaller MZs, with unequal sizes. The ability to estimate water status using thermal images is assumed to be affected by the size of the MZ, thus influencing the efficiency of variable rate irrigation decisions at small scales. In this study, the effectiveness of CWSI as a predictor of Ψ_{stem} across decreasing sizes of areas of interest within a vineyard was assessed. The aim was to determine the minimum scale size for its potential application in precision irrigation.

Apart from the absence of consideration for the spatial scale effect, there appears to be a predominant oversight regarding temporal effects influencing the efficacy of CWSI in predicting Ψ_{stem} . Previous studies showed that seasonality was a major factor in the prediction of water consumption and yield components of grapevines (Ohana-levi et al., 2020; 2022; 2024). Nevertheless, despite the demonstrated errors originating from various sources in CWSI- Ψ_{stem} relationships, there has been limited investigation into the robustness of the model in multi-year studies (Bellvert et al., 2014a). This study aims to address this gap by examining the robustness of CWSI- Ψ_{stem} relationships over four seasons.

To encapsulate, the study aimed to fill three pivotal knowledge gaps: (1) determining the superior representation of vineyard water status—whether it is Ψ_{stem} , characterized by high accuracy but low sample size as employed in current practical water status monitoring, or CWSI, possessing lower accuracy but greater spatial representation; (2) identifying the optimal scale for effectively representing vine water status using CWSI for precision irrigation; and (3) understanding the impact of the season on the CWSI- Ψ_{stem} relationship, as well as determining the number of seasons required to establish a reliable and robust Ψ_{stem} prediction model based on CWSI and additional meteorological parameters.

Table 1 Previous studies presenting aerial based CWSI and Ψ_{stem} or Ψ_{leaf} regressions in vineyards

References	Region, country	Research plot size (ha)	Vines per ha	Variety*	Measurement type	Vines measured	Vines measured (%)	Measurement days	Seasons	Irrigation treatment	Ψ_{stem} range (MPa)	R ²
Baluja et al., (2012)	Rioja, Spain	5	2976	Temp.	Ψ_{stem}	30	0.20	1	1	No	1–1.5	0.5
Bellvert et al., (2014a, 2014b)	Lleida, Spain	11	1897	PN	Ψ_{leaf}	18	0.09	6	2	No	0.55–1.7	0.57
		22	1666	Char.	Ψ_{leaf}	18	0.05	6	2	No	0.55–1.7	0.72
		18.4	1666	Syra	Ψ_{leaf}	18	0.06	6	2	No	0.55–1.7	0.75
		14.5	1666	Temp.	Ψ_{leaf}	18	0.07	6	2	No	0.55–1.7	0.56
Bellvert et al., (2016a, 2016b)	Lleida, Spain	16	1667	Char.	Ψ_{leaf}	48	0.18	14	1	yes	0.5–1.3	0.61
Sepúlveda-Reyes et al., (2016)	Maulle, Chile	0.00075	2666	Carménè	Ψ_{stem}	32	100	8	1	yes	0.65–1.9	0.36
Santesteban et al., (2017)	Navarra, Spain	7.5	3333	Temp.	Ψ_{stem}	70	0.28	1	1	No	0.45–0.9	0.69
Bahat et al. (current)	Judean hills, Israel	0.0009	2222	Cab.	Ψ_{stem}	2	100	22	4	No	0.55–1.99	0.51
		0.09				6	3				0.65–1.9	0.65
		0.61–0.96				20–56	2.1				0.8–1.5	0.67
		0.9				60	3				0.8–1.55	0.82
		1.8				120	3				0.85–1.55	0.88

*Grapevine varieties: Tempranillo (Temp), Pino-noir (PN), Chardonnay (Char), Cabernet sauvignon (Cab)

Materials and methods

Study site

The study was conducted from 2017–2020 in a commercial vineyard of *Vitis vinifera* L. ‘Cabernet Sauvignon’ grafted onto 101–14 rootstock in Mevo-Beitar, Israel (31°43' N; 35°06' E; Fig. 1). The vine spacing was 1.5 m within rows and 3 m between rows (2222 vines per hectare), and the whole vineyard consisted of 5522 vines. The vines were planted in 2011, with a row direction of 117°–297°, and were trained to a vertical shoot positioned trellis system with two foliage wires on each side.

The vineyard was delineated into 20 management cells (MCs; referred by the letters A–T), and three pairs of vines per MC (60 pairs; 120 vines in total) were selected as measurement vines.

Description of scales

Five different scales with increasing polygon sizes were selected for this study: (1) Measurement vines (MV)—two adjacent vines, (2) Management cells (MC)—a polygon of 30×30 m consisting of ~200 vines, (3) Management zones (MZ)—a natural delineation of the vineyard based on topography attributes (Bahat et al., 2021), (4) Irrigation blocks—2 sub-units of the vineyard irrigated by different valves, and (5) The entire vineyard. Scales are further detailed in Table 2.

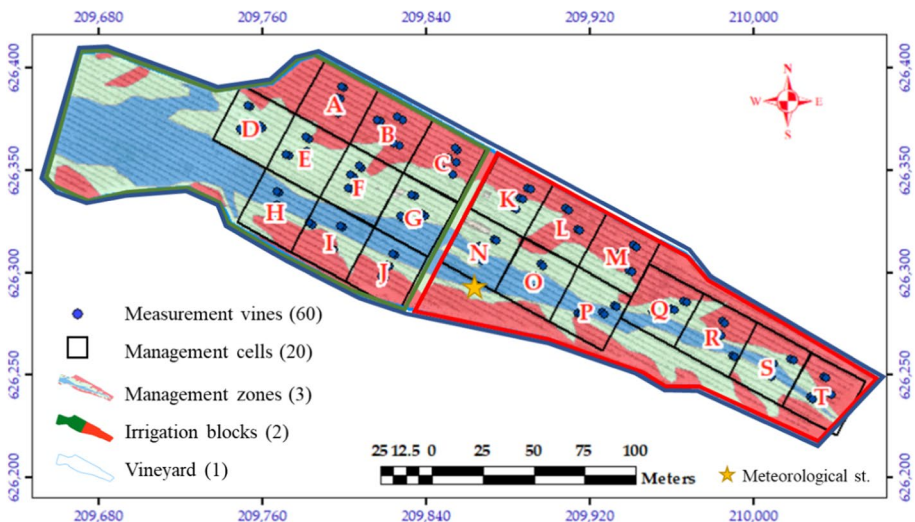







Fig. 1 Mevo-Beitar experimental vineyard. Measurement vines are represented by blue dots ($n=60$), management cells are represented by black squares with different letters ($n=20$), management zones are represented by the colored (red, green, and blue) polygons overlaying the vineyard, irrigation blocks are a division of the western and eastern sections of the vineyard, and the total vineyard area is represented by a blue polygon. In brackets is the number of repetitions per measurement day for each scale (Color figure online)

Table 2 Scales description at the vineyard, Mevo-Beitar, Israel

#	Sign	Unit	Abbr.	Number of repetitions	Name	Polygon size	Number of vines measured (Ψ_{stem})	Percentage of vines measured
1		Measurement vines	MV	60	A1 -T3	9m ²	2	100% (2/2)
2		Management cells	MC	20	A -T	900m ²	6	3% (6/200)
3		Management zones	MZ	3	MZ1 (red) MZ2 (green) MZ3 (blue)	9139m ² 9567m ² 6142m ²	44 56 20	2.2% (44/2031) 2.6% (56/2126) 1.5% (20/1365)
4		Irrigation blocks	–	2	East, West	1.25ha	60	2.2% (60/2761)
5		Vineyard	–	1	–	2.5ha	120	2.2% (120/5522)

Data collection and analysis

Twenty-two campaigns were undertaken during the 2017–2020 seasons (Table 3). All measurements were done on sunny, cloudless days during the growing season. Measurements were taken simultaneously around noon between 11:45–14:30, including mid-day stem water potential (Ψ_{stem}) of 120 vines using a pressure chamber and remote sensing measurements using a UAV with a triple payload of thermal camera, multispectral camera and RGB camera. The spatially intensive Ψ_{stem} measurements of 120 vines was regarded as the benchmark ("gold-standard"), intended for comparison with alternative measurements and modeling approaches.

Vine water status

In Israeli commercial vineyards, Ψ_{stem} is typically measured on four or six vines per plot, at two or three spots within the vineyard (Helman et al., 2018). As previously stated, this study involved measuring Ψ_{stem} for all 120 measurement-vines (denoted as $\Psi_{\text{stem}120}$) to provide a comprehensive representation of the water status across the entire vineyard and serve as a benchmark ("gold-standard"). Ψ_{stem} was measured around solar noon (12:00–14:30 Israel standard time). The measurements were conducted using pressure chambers (model Arimad 3000, MRC, Holon, Israel) according to the procedure of Boyer (1995). A mature, fully expanded leaf from each measurement vine was bagged 2 h prior to acquisition with aluminum and plastic bags. The time elapsing between leaf excision and chamber pressurization was less than 20 s.

Crop water stress index

Crop water stress index (CWSI) was based on canopy temperature (Jackson et al., 1981). Thermal data were acquired between 11:45–12:00 Israel standard time at the same day of Ψ_{stem} measurements. An airborne FLIR SC655 thermal camera was used to evaluate the vineyard's canopy surface temperature. The camera (FLIR® Systems, Inc., Billerica, MA, USA) provided images of 640 pixels \times 480 pixels, with a spectral range sensitivity of 7.5–13 μm and a measurement accuracy of ± 0.5 $^{\circ}\text{C}$ in the temperature range of the vineyard. The images were acquired from 100 m above ground level with a 24 mm lens, resulting in a ground spatial resolution of 6.7 cm/pixel. The flight plan included 70% overlap between adjacent legs, and 90% overlap in the flight direction. Seven ground control points were placed within the scanned area, and their geographical coordinates were measured using an RTK GPS, with 1 cm accuracy. The mosaic produced was georeferenced from the acquired images using Pix4d commercial software (Pix4D, Prilly, Switzerland).

Equation 1 was used to calculate CWSI (Jackson et al., 1981):

$$\text{CWSI} = \frac{T_{\text{canopy}} - T_{\text{wet}}}{T_{\text{dry}} - T_{\text{wet}}}, \quad (1)$$

where T_{canopy} is the temperature of the canopy, T_{wet} is the temperature of a theoretical fully transpiring canopy and T_{dry} is the temperature of a theoretical non-transpiring canopy. T_{canopy} was acquired for polygons at all five scales (Table 2), and the coolest 33% of the pixels within each of the polygons were averaged following Meron et al. (2010). T_{wet} was calculated at the vineyard scale using the average temperature of the coolest 5% of the canopy pixels (Cohen et al., 2017; Rud et al., 2014). For T_{dry} calculation, the warmest 15% of

Table 3 Data acquisition campaign dates, phenological stage, thermal pixel size, Ψ_{stem} and meteorological data for each measurement day

Serial number	Date	Growth stage	Pixel size (cm)	Ψ_{stem} avg (MPa)	Ψ_{stem} range (MPa)	VPD (kPa)	Cumulative ET_0 (7d; mm)	Cumulative ET_0 (from anthesis; mm)	Solar radiation (W/m^2)
1	19 Jul 2017	2	6.87	-1.14	0.557	2.2	44.94	478.5	938.1
2	9 Aug 2017	3	6.97	-1.44	0.519	3.2	41.22	604.4	907.9
3	5 Sep 2017	3	6.82	-1.53	0.903	3.2	35.16	751.1	831.3
4	4 Jul 2018	2	6.82	-1.00	0.445	2.8	42.47	364.4	1003.7
5	18 Jul 2018	2	6.82	-1.04	0.449	3.5	41.11	450.6	1011.0
6	31 Jul 2018	3	6.82	-1.10	0.537	2.5	42.51	529.4	989.0
7	29 Aug 2018	3	6.82	-1.38	0.656	3.3	34.61	683.0	924.5
8	5 Jun 2019	1	6.82	-0.84	0.301	3.5	48.08	216.1	971.6
9	24 Jul 2019	2	6.82	-0.91	0.424	3.3	42.18	509.4	992.6
10	21 Aug 2019	3	6.82	-1.05	0.573	2.4	39.46	674.0	943.8
11	28 Aug 2019	3	6.82	-1.18	0.645	2.3	38.13	712.2	911.3
12	4 Sep 2019	3	6.82	-1.16	0.651	2.1	36.62	748.8	902.1
13	11 Sep 2019	3	6.82	-1.23	0.512	2.3	32.56	781.3	887.1
14	17 Jun 2020	2	6.82	-0.88	0.198	3.5	42.84	277.3	1012.2
15	1 Jul 2020	2	6.75	-0.95	0.316	2.7	41.49	358.5	986.9
16	15 Jul 2020	2	6.89	-1.00	0.484	2.8	40.28	442.5	988.6
17	22 Jul 2020	2	6.85	-1.09	0.543	2.9	41.62	484.1	988.8
18	5 Aug 2020	3	6.79	-1.17	0.715	2.2	41.87	567.2	941.3
19	19 Aug 2020	3	6.85	-1.30	0.712	2.7	39.27	642.8	953.6
20	26 Aug 2020	3	6.78	-1.23	0.781	2.7	37.8	680.6	937.0
21	2 Sep 2020	3	6.81	-1.31	0.799	2.9	37.16	717.8	888.1
22	8 Sep 2020	3	6.88	-1.33	0.907	2.5	38.43	751.1	850.8

Growth stage was determined after (Coombe & McCarthy, 2000), cumulative ET_0 (7d) referred to the accumulated ET_0 7 days before acquisition date

the canopy pixels were averaged at the vineyard scale following Bian et al. (2019). T_{canopy} , T_{wet} and T_{dry} were calculated using the “raster” package in R (Hijmans et al., 2020).

Image processing for pure canopy extraction included the following three major steps: (1) A temperature threshold of 45 °C was determined by visual analysis of the temperature bimodal histogram to remove soil-associated pixels. (2) The irrigation lines GIS layer was used to create a 0.8 m width linear layer around the vine rows using the buffer tool in ArcMap 10.6 (ESRI Inc. Redlands, CA, USA). (3) An NDVI threshold was used to mask non-crop pixels other than soil. For that, multi-spectral images in the VIS–NIR were acquired using a MicaSense multispectral camera RedEdge MX (MicaSense® Inc, Seattle, WA, USA) with five sensors (blue: 465–485 nm, green: 550–570 nm, red: 663–673 nm, red edge: 712–722 nm, and near infrared: 820–860 nm). An external irradiance sensor with GPS and inertial measurement unit (IMU) was placed on top of the UAV to capture sensor angle, sun angle, location, and irradiance for each image during flight. The normalized difference vegetation index (NDVI) was calculated using red and near infrared (NIR) bands according to:

$$\text{NDVI} = \frac{\rho(\text{NIR}) - \rho(\text{Red})}{\rho(\text{NIR}) + \rho(\text{Red})}, \quad (2)$$

where $\rho(\text{NIR})$ is the reflectance value for near infrared band (center wavelength 0.840 μm) and $\rho(\text{Red})$ is the reflectance value for the visible red band (center wavelength 0.668 μm). NDVI values range between 0 and 1. For masking other non-canopy pixels (mostly shade and grass), an NDVI image was used from the same campaign to indicate pixels with values above an empirical threshold of 0.3. All three steps were performed automatically using the ModelBuilder programming tool in ArcMap 10.6 (ESRI Inc. Redlands, CA, USA).

Meteorological data

Reference evapotranspiration (ET_0) was calculated according to the FAO Penman–Monteith equation (Allen et al., 2006) from a meteorological station located six km from the vineyard (Tzuba meteorological station, 31.78° N; 35.12° E). In addition, a portable meteorological station was positioned at canopy height within the vineyard, which recorded the temperature, relative humidity, and solar radiation during all hours of data collection to a data logger (Campbell Scientific, Logan, UT, USA). The presented solar radiation was averaged from data acquired between 11:45–12:00 Israel standard time.

CWSI- Ψ_{stem} regression models

Ψ_{stem} was assessed by either single linear regression based on CWSI, or by multi-variate linear regression based on CWSI and additional meteorological parameters. To assess the accuracy of the models at five different scales, statistical data including adjusted determination coefficient (R^2 adj) and root mean square error (RMSE) were obtained for the predicted Ψ_{stem} values. A stepwise regression model was implemented with a mixed, minimum AICc stopping rule to create a four-parameter model.

To assess the influence of each individual independent variable on Ψ_{stem} estimation a dominance analysis was performed. Dominance analysis estimates the relative importance of predictors by examining the change in R^2 of the regression model from adding one predictor to all possible combinations of the other predictors (Budescu, 1993). In our case 15

subset regressions were examined for each of the scales, to decompose the effect of each variable. The final four-parameter model consisted of: CWSI as a spatial variable, solar radiation as a temporal variable, accumulated ET_0 from anthesis as a long-term seasonal drought stress variable, and accumulated ET_0 of the last 7 days before the campaign as a short-term drought stress variable.

Model performance

The accuracy of the model was evaluated by forming sub-models with partial data sets (one, two or three seasons) and implementing them on a test set from another season (or seasons). In most studies, cross validation is applied by randomly dividing data into calibration, validation and test (Gutiérrez et al., 2018; Romero et al., 2018). In this study, a conservative method was used by taking complete seasons as test cases. Fifty models were created and were separated into six calibration/test ratios (Table 6). For example, in the case of three seasons (calibration set) that predicted a single season (test set; 3p1), four different models were formed (2017, 2018, 2019 predicting 2020; 2018, 2019, 2020 predicting 2017; 2017, 2018, 2020 predicting 2019; and 2017, 2019, 2020 predicting 2018). Model performance was evaluated and tested at the MC scale using averaged R^2 and averaged RMSE. To compensate for the decreasing number of observations between scales and variables number between models, an adjusted R^2 was calculated.

Prediction of irrigation decisions and Ψ_{stem}

The models were validated using two methods: (1) calculation of the averaged absolute distance of predicted Ψ_{stem} values to the measured Ψ_{stem} values (RMSE), and (2) analysis of irrigation decision errors using a "what-if-analysis" of the irrigation model with increasing irrigation levels based on Ψ_{stem} thresholds. The irrigation model was based on lysimeter-derived crop evapotranspiration (ET_c), weekly field LAI measurements (Munitz et al., 2019; Netzer et al., 2009), and ET_0 . At all fruit development stages, the basic irrigation factor was 0.2 of the calculated ET_c . Ψ_{stem} measurements were used to adjust the irrigation factor as described by Bahat et al. (2019).

Three different methods were used to predict Ψ_{stem} at the vineyard scale for each measurement day.

- 1) $\Psi_{stem}4$, involves measuring Ψ_{stem} in 4 vines from 2 locations in the vineyard selected by the viticulturist. This method simulated water status monitoring typically practiced in large wineries.
- 2) $\Psi_{stem}6$, involves measuring Ψ_{stem} in 6 vines from 3 locations in the vineyard selected by the viticulturist. This method simulated water status monitoring typically practiced in boutique wineries.
- 3) The 3p1 model was based on thermal and meteorological parameters.

All three methods were compared to the mean $\Psi_{stem}120$ "gold-standard".

Further analysis assessed the potential for accurately estimating Ψ_{stem} at the management cell (MC) scale to determine the feasibility of implementing precision irrigation and its potential advantages over uniform irrigation practiced by thermal-based estimated Ψ_{stem} . The CWSI-based model at the MC scale, enhanced with meteorological variables, was utilized to predict Ψ_{stem} for each MC on every imaging date. Subsequently, the mean

estimated Ψ_{stem} for each MC on each date was compared to the corresponding mean Ψ_{stem} directly measured in 6 vines per MC (used as a benchmark). The Absolute error for each MC was then calculated and mapped. Additionally, the estimated Ψ_{stem} ($\Psi_{\text{stem}120\text{est}}$) values based on the whole vineyard model for each date were compared to the benchmark, i.e., the mean Ψ_{stem} values directly measured in 6 vines per MC, and the absolute error for each MC was calculated and mapped. Finally, the two error maps were compared.

Statistical data analysis was performed using JMP software (Pro 16, SAS Institute, Cary, NC, USA) and R software (R Core Team, 2019).

Results

CWSI- Ψ_{stem} regression models

Results of predicted (based on CWSI) vs. observed Ψ_{stem} are shown in Fig. 2 for each scale, and their R^2 and RMSE are shown in Fig. 2f. Model RMSE decreased as scale size increased, yet showing no variation between the two largest scales. i.e., irrigation blocks and the whole vineyard. R^2 ranged between 0.36 and 0.57.

Adding meteorological parameters to the prediction of Ψ_{stem} based on CWSI improved model performance compared to the model based solely on CWSI (Figs. 2 and 3). RMSE decreased from a range of 0.12–0.24 for the CWSI based model to 0.07–0.18 for the four-parameter model. R^2 improved from 0.36–0.57 to 0.51–0.85, respectively. The slope of the regression curve was closer to 1 for the four-parameter model indicating better model calibration compared to the model based solely on CWSI. The accuracy of the four-parameter model improved with increasing scale size, from MV scale

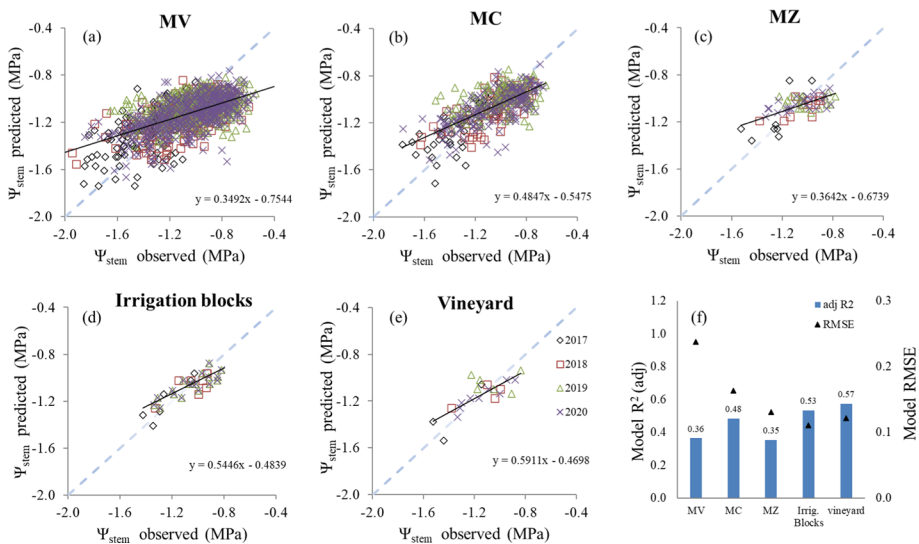


Fig. 2 Observed Ψ_{stem} against predicted Ψ_{stem} (using only CWSI) in 2017–2020 for **a** measurement vines (MV), **b** management cells (MC), **c** management zones (MZ), **d** irrigation blocks and **e** entire vineyard. **f** R^2 and RMSE for each of the scales

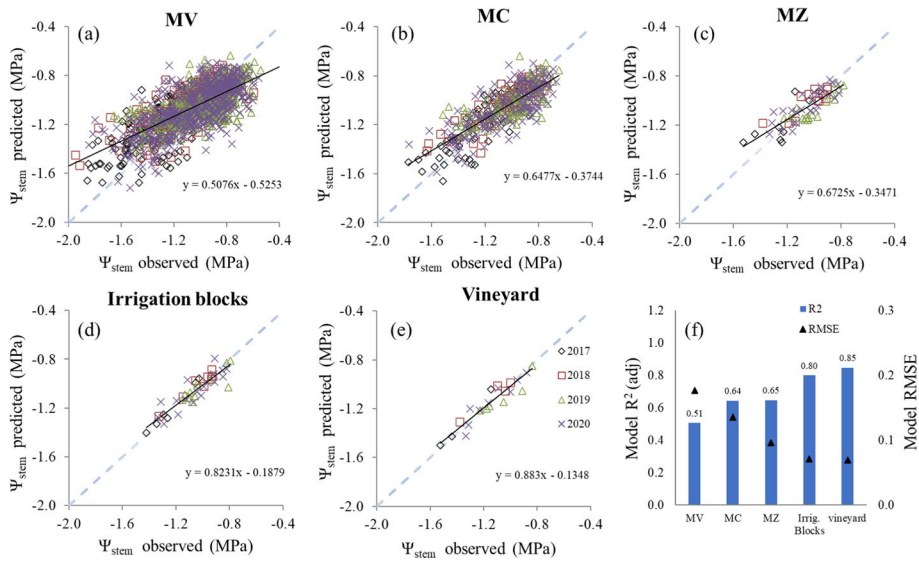
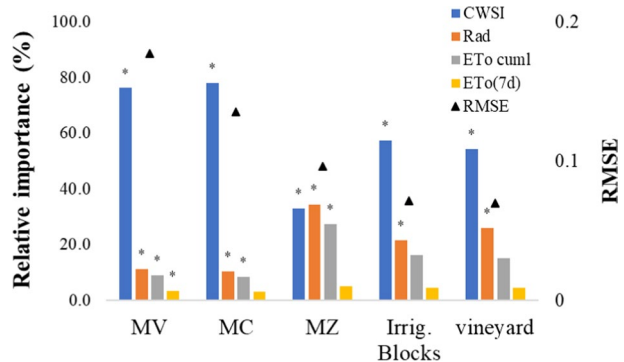


Fig. 3 Actual Ψ_{stem} against predicted Ψ_{stem} in 2017–2020 for **a** measurement vines (MV), **b** management cells (MC), **c** management zones (MZ), **d** irrigation blocks and **e** entire vineyard. The variables that were considered in the model were CWSI, solar radiation, cumulative ET_0 of previous 7 days and the cumulative ET_0 from anthesis. **f** R^2 and RMSE for each of the scales presented.

to the irrigation block scale. Similarly to the trend that was observed with the model based solely on CWSI (Fig. 2), no improvement was shown from irrigation blocks to the vineyard scale.

In the four-parameter model, CWSI had the highest contribution to the prediction of measured Ψ_{stem} , ranging from 33 to 78% across the different scales (Fig. 4). Solar radiation contributed 10–34%, and this contribution, like that of CWSI, was statistically significant at all five scales. ET_0 cuml contributed significantly to the prediction of Ψ_{stem} at the three smallest scales and ET_0 7d only at the smallest, MV scale.

Fig. 4 Dominance analysis and root mean square error (RMSE) for the variables used in the four-season regression model. The X-axis is arranged from the smallest to the biggest scale (i.e., MV is the smallest and vineyard is the largest scale). RMSE is shown in black triangles, bars with different colors represents the relative importance of the variables. Asterisks represent the level of statistical significance (p -value < .05)



Model validation at the vineyard scale

Substantial differences were observed among $\Psi_{\text{stem}6}$, $\Psi_{\text{stem}4}$, and the 3p1 model (Table 4). $\Psi_{\text{stem}6}$ and $\Psi_{\text{stem}4}$ exhibited 5 and 6 irrigation errors, respectively, whereas the 3p1 model experienced only 3 irrigation errors. The disparities among them extended as indicated by the RMSE. The 3p1 model demonstrated a mean error of 0.07 MPa, while $\Psi_{\text{stem}6}$ and $\Psi_{\text{stem}4}$ showed errors of 0.18 and 0.24 MPa, respectively.

Model validation at the MC scale

Model performance estimation

Sets of three (3p1) or two (2p2, 2p1) seasons better predicted Ψ_{stem} in an additional season (Fig. 5) as indicated by their relatively high R^2 and low RMSE compared to other combinations (1p2, 1p1, 1p3). The 3p1 combination was most accurate (Table 6, Appendix).

Model prediction of irrigation decisions and Ψ_{stem}

On each campaign date, a validation was performed by comparing the irrigation decision based on the 3p1 model to that based on the measured $\Psi_{\text{stem}120}$. Irrigation decisions were accurate 79.3% of the time (Table 5). Overall, 15.5% of the model decisions led to under-irrigation and 5.2% of the decisions led to over-irrigation. Most of errors occurred at campaign dates early in the season.

Spatial representation of Ψ_{stem} at the MC scale

Using the 3p1 MC models (Fig. 3b) for Ψ_{stem} prediction on each date yielded more accurate water status estimations at the MC scale (lower absolute error; Fig. 6, left) compared to the $\Psi_{\text{stem}120_{\text{est}}}$ uniform means from the 3p1 whole-vineyard models (Figs. 3e and 6, right). The enhanced prediction is particularly significant given the inferior performance of the 3p1 MC models compared to the 3p1 whole-vineyard models. Note that the absolute errors for the western block (A–J) tended to be higher than that of the eastern block (K–T).

Discussion

Current best management practice to evaluate water status in a commercial vineyard to support irrigation decisions is done by direct measurement of Ψ_{stem} in a few, supposedly representative, number of vines (Helman et al., 2018). As expected, this current water status monitoring under-represented the spatial variability of the vineyard in the current study. An alternative is to use remotely-sensed products depicting indirect, and necessarily less accurate and less reliable information, but from all vines. This trade-off exists in a variety of sensing utilizations in many disciplines, as well as in agriculture and in particular in precision agriculture (Cai & Zhu, 2015; Kamilaris et al., 2017). Previous studies examined various sources of errors that compromise the ability of CWSI to estimate water status (Gonzalez-Dugo & Zarco-Tejada, 2022; Jones & Sirault, 2014; Pou et al., 2014). Yet, based

Table 4 Errors of three different methods of calculating Ψ_{stem} at the vineyard scale: (1) Ψ_{stem6} —averaged Ψ_{stem} of six vines from three locations (simulating the practice in boutique wineries), (2) Ψ_{stem4} —averaged Ψ_{stem} of four vines from two locations (simulating the practice in large wineries), and (3) 3pl model— Ψ_{stem} predicted from the thermal 3pl model

Date	Ψ_{stem6} error (MPa)	Ψ_{stem4} error (MPa)	3pl model error (MPa)	$\Psi_{stem120}$ irrigation decision	Ψ_{stem6} irrigation decision	Ψ_{stem4} irrigation decision	3pl_model irri- gation decision
19 Jul 2017	0.23	0.30	0.14	0	0	0	0
9 Aug 2017	0.16	0.17	0.06	0.2	0	0	0.2
5 Sep 2017	0.44	0.54	0.07	0.2	0	0	0.2
4 Jul 2018	0.21	0.23	0.03	0	0	0	0
18 Jul 2018	0.17	0.29	0.01	0	0	0	0
31 Jul 2018	0.24	0.22	0.11	0	0	0	0
29 Aug 2018	0.38	0.39	0.10	0	0	0	0
5 Jun 2019	0.01	0.08	0.00	0.4	0.4	0.3	0.4
24 Jul 2019	0.06	0.20	0.19	0	0	0	0
21 Aug 2019	0.07	0.14	0.16	0	0	0	0
28 Aug 2019	0.15	0.25	0.08	0	0	0	0
4 Sep 2019	0.12	0.27	0.09	0	0	0	0
11 Sep 2019	0.17	0.21	0.03	0	0	0	0
17 Jun 2020	0.02	0.02	0.04	0.2	0.2	0.2	0.3
1 Jul 2020	0.24	0.17	0.04	0.2	0	0	0.2
15 Jul 2020	0.24	0.25	0.06	0	0	0	0
22 Jul 2020	0.16	0.22	0.07	0	0	0	0
5 Aug 2020	0.24	0.31	0.02	0	0	0	0
19 Aug 2020	0.21	0.27	0.12	0.2	0	0	0
26 Aug 2020	0.13	0.18	0.03	0	0	0	0
2 Sep 2020	0.30	0.42	0.03	0.2	0	0	0.2
8 Sep 2020	0.06	0.17	0.11	0	0	0	0.2
RMSE	0.18	0.24	0.07	Irrigation mistakes		5	3

Ψ_{stem} error (left; MPa) and irrigation errors (right) were derived from the measured 120 vines

Bold indicates under-irrigation and Bolditalic over-irrigation

on a literature review, no previous study examined whether CWSI-generated products were better or worse than current water status manual monitoring alternatives. Additionally, no study determined the minimal size for which the CWSI product would be reliable. Furthermore, from a temporal aspect, the robustness of the relationships of CWSI and Ψ_{stem} , which determine the quality of the water status estimation, has hardly been addressed.

Vineyard water status: UAV-thermal-based maps vs. laborious monitoring of a few vines

The thermal based model tested in the current study was found to provide better estimation of vineyard water status compared to standard Ψ_{stem} measurements from either four or six vines when compared to the extensive highly dense Ψ_{stem} measurements from 120 vines (Table 4). In this study, a model was created using a conservative validation, in which three seasons were used for data calibration and another season served as a test set (3p1). The 3p1 model presented higher accuracy (RMSE=0.07), compared to current water status manual monitoring accuracy (RMSE=0.18–0.24) and had only three irrigation errors compared to five to six errors for the current water status manual monitoring Ψ_{stem} measurement (Table 4). It should be stressed that Ψ_{stem} prediction was done using data from different seasons that was compared to current daily Ψ_{stem} measurements, reinforcing the model's robustness. This comparison is part of the inherent trade-off between a rapid, spatial water status measurement of the entire vineyard (i.e., all vines), and an accurate, pinpointed, low sample size water status measurement. The superiority of the Ψ_{stem} estimated by thermal imaging at stages II and III of fruit development means that it can be incorporated first and foremost for an in-season water status assessment program at the vineyard scale and improve commercial uniform irrigation. At early phenological stages, however, the model accuracy was found significantly lower (Fig. 7, Appendix) possibly due to errors stemming from varying atmospheric conditions (Sepúlveda-Reyes et al., 2016), and from seasonal modification of the relationships between leaf stomatal conductance and Ψ_{stem} (Herrera et al., 2022). It may be argued that inferiority of the manual monitoring of Ψ_{stem} that resulted in subpar spatial representation is attributed to the sampling locations (i.e. 2 or 3 pairs of vines in close proximity) and enhancement potentially be achieved through optimizing the distribution of sampling. Several recent studies have proposed methodologies to optimize sampling locations by integrating ancillary data. These studies have implemented such optimization across diverse domains, including multifunctional-matching-based approach for any target value or measurement (Ohana-Levi et al., 2021), the strategic deployment of moisture sensors (Arno et al., 2023), and for yield sampling in vineyards (Oger et al., 2021). However, in our opinion, these methods are more aptly suited for determining sensor locations, and may be less applicable to periodic measurements that necessitate physical presence within a short timeframe, as is the case with Ψ_{stem} measurements.

What is the smallest scale that at which CWSI effectively represents vine water status for precision irrigation?

Beyond the ability to well represent water status at the vineyard scale this study also aimed at identifying the optimal scale for effectively representing vine water status using CWSI for precision irrigation. The rationale to reduce the measured area from a vineyard scale to the single vine scale stems from the precision agriculture approach that promotes

Fig. 5 Model accuracy attributes with different number of seasons used for calibrating and testing Ψ_{stem} values. The calibration/test ratio is shown on the X-axis. E.g., 3p1 means that three seasons of data were used to predict a single season of Ψ_{stem} values. The total number of model combinations was four. The Y-axis depicts the averaged R^2 (orange rectangles) and the RMSE (blue triangles) (Color figure online)

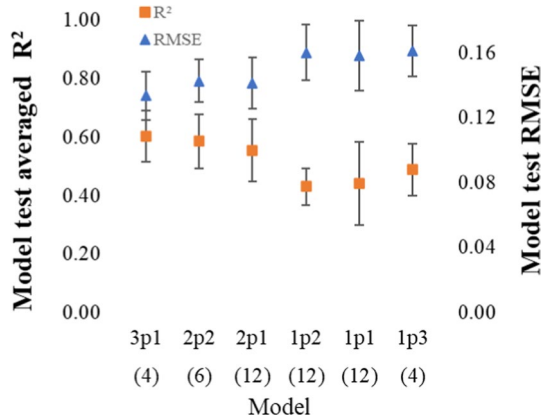


Table 5 RMSE of Ψ_{stem} and irrigation decisions errors at the management cell scale (n = 440 combinations of 20 MCs and 22 measurement days), using the 3p1 model

Date	Ψ_{stem} predicted RMSE (MC)	Irrigation decisions		
		Correct	Under	Over
19 Jul 2017	0.112	19	1	0
9 Aug 2017	0.102	14	4	2
5 Sep 2017	0.134	11	7	2
4 Jul 2018	0.069	20	0	0
18 Jul 2018	0.061	20	0	0
31 Jul 2018	0.083	20	0	0
29 Aug 2018	0.129	13	6	1
5 Jun 2019	0.074	11	5	4
24 Jul 2019	0.151	20	0	0
21 Aug 2019	0.103	18	2	0
28 Aug 2019	0.107	16	4	0
4 Sep 2019	0.119	16	4	0
11 Sep 2019	0.111	19	1	0
17 Jun 2020	0.073	9	8	3
1 Jul 2020	0.093	13	2	5
15 Jul 2020	0.135	15	2	3
22 Jul 2020	0.135	14	5	1
5 Aug 2020	0.102	17	3	0
19 Aug 2020	0.143	14	6	0
26 Aug 2020	0.116	18	2	0
2 Sep 2020	0.135	16	4	0
8 Sep 2020	0.129	16	2	2
RMSE	0.11	Sum of decisions 349 (79.3%)	68 (15.5%)	23 (5.2%)

For each date, 20 irrigation decisions, separated into correct, under-irrigation and over-irrigation decisions compared to the irrigation decision based on Ψ_{stem} 120

RMSE of predicted Ψ_{stem} was calculated as the average of 20 management cells for each date

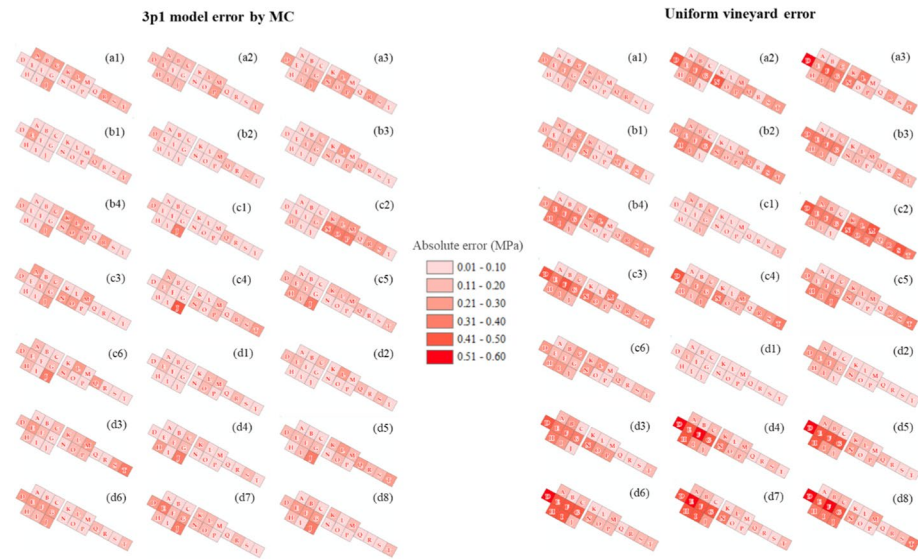


Fig. 6 Absolute error of Ψ_{stem} at the MC scale for all dates across the four seasons – 2017 (a1–a3), 2018 (b1–b4), 2019 (c1–c6) and 2020 (d1–d8). In the left side is the absolute error of differential Ψ_{stem} for every MC estimated by the MC 3p1 model. In the right side is the absolute error of a uniform $\Psi_{\text{stem}120_{\text{est}}}$ used for all 20 MCs estimated by the whole vineyard 3p1 model. Ψ_{stem} values measured at 6 vines per MC were used as benchmarks to calculate the absolute error

site-specific solutions. It can be expected that the ability to predict Ψ_{stem} at the smallest scale (MV), where the percentage of the measured vines in the imaged polygon was 100% (Table 2) will be more precise than scales with substantially lower representation rate of vines. For example, several studies (e.g., Cohen et al., 2005; Moller et al., 2007; Grant et al., 2007) compared Ψ_{leaf} or Ψ_{stem} of the same leaves used in high-resolution thermography to calculate CWSI to avoid variations stem from the intra-canopy variability. In the current study it was found that at the MV scale, model accuracy was the lowest. The reason for this is likely the smaller of what can be called "signal-to-noise ratio" (SNR; Atkinson et al., 2007) compared to the other scales. At the MV scale, T_{canopy} was assessed using only few hundred pixels, while on the next size scale, the MC, about 50,000 pixels were used. Moving to the largest vineyard scale, yielded roughly 1 million pixels that were used. It is assumed that the large number of pixels allowed greater noise reduction by removing more of the non-canopy pixels. In this way, a larger proportion of pure canopy pixels was accounted for in the final determined value of T_{canopy} . It should be mentioned that, at each of the scales, a separate calculation of CWSI was performed and the pure canopy pixel selection was made independently.

These results contradict Cohen et al. (2005) who measured single cotton leaves and presented high CWSI- Ψ_{leaf} model accuracy, probably due to the fact that they used very high spatial resolution of thermal pixels (0.5 cm per pixel) allowing precise measurement of a single leaf, thus increasing the signal within the image. Similarly, Grant et al. (2007) measured vines canopy using a thermal camera mounted on a tripod perpendicular to the imaged area at a very high (sub-centimeter) spatial resolution to distinguish between irrigation treatments. There is room for more in-depth research on the subject that will further evaluate similar scale sizes with different pixel numbers.

Despite the reduction in model accuracy as a function of decreasing scale size (Fig. 3) water status evaluation at the small MC scale using the MC scale model (Fig. 3b) produced a substantially lower Ψ_{stem} error compared to whole vineyard scale single rate evaluation (Fig. 6). This is expected to allow superior irrigation decisions for small-scale management zones in vineyards practicing precision irrigation. These findings align with results observed in other precision irrigation experiments. (Cohen et al., 2021) demonstrated that variable rate drip irrigation (VRDI) in cotton improved water use efficiency without compromising yield. Ortuani et al. (2019) illustrated a reduction of water use when comparing a reference plot (following traditional farmer practices) in vineyards. Sanchez et al. (2017) similarly showed that VRDI management led to increased yield and water use efficiency in vineyards, and Katz et al. (2022) found that Ψ_{stem} was better maintained under VRDI compared to uniform irrigation in peaches. Comprehensive insights into the challenges associated with implementing precision drip irrigation were provided by Ben-Gal et al. (2022). However, recently possible technological solutions have been developed including the development of a smart dripper with multiple statuses (Alchanatis & Shkolnik, 2023), and implementation of wireless communication among water valves, each controlling specific sub-areas in the field (Shaked, 2023). Although these technologies are still in their infant stages, they lay the groundwork for the prospective application of VRDI in the near future, enhancing the practical relevance of the findings from this study.

This study investigated how altering the target area of interest—without changing the original high resolution of the UAV image and without considering the spatial structure of water status as reflected by the Ψ_{stem} —affects the accuracy of estimating Ψ_{stem} using thermal UAV. Tisseyre et al. (2018) have found that the grid size is dependent on the resolution of the available information and the spatial structure of the raw data. Our research demonstrated the feasibility of accurately representing the water status down to a minimal area of a management cell that in our study was set to 30×30 m. Nevertheless, the absolute magnitude appears to be influenced by both the image resolution and the spatial structure of the water status. There is potential to explore combinations of resolutions and spatial structures to determine the minimum absolute size for each combination but it was beyond the scope of this study. However, it is reasonable to assume that the identified trend persists; with a specific resolution of the UAV image, reducing the target area leads to a decrease in the signal-to-noise ratio until the point where the assessment of water status falls below the desired accuracy.

Model accuracy and robustness over time

Model accuracy and robustness can be evaluated using a separate dataset comprised of samples from different place and time. Several methods are available with cross-validation, leave-one-out, and k-fold frequently used for model validation (Berrar, 2018). Annual oscillations of grapevine physiology and wine quality are commonly reported in vineyards (Jones et al., 2005; Ohana-Levi, et al., 2020) and therefore should be accounted for in model building and validation. In this study, the models were created using a conservative validation, in which whole seasons were used for data calibration and for testing. The thermal-based water status model was assumed to be not scalable (i.e., a valid model of one vineyard will not necessarily fit another vineyard), therefore we evaluated the number of seasons required for establishing a valid model in a single vineyard (Fig. 5). The minimal time required for establishing such a model was found to be two seasons.

The findings regarding improved model prediction due to addition of meteorological parameters (Figs. 2 and 3) suggest that the seasonality effect of water status prediction was mitigated by considering the changes in conditions between campaign days and the cumulative evaporative demand that differed between seasons (Table 3). Solar radiation was the most important contributor to the prediction of Ψ_{stem} after CWSI (Fig. 4). The approach adopted in this study, and commonly used in other studies (Gonzalez-Dugo & Zarco-Tejada, 2022; Grant et al., 2007; Möller et al., 2007), majorly aims at calibrating the effects of air temperature and vapor pressure deficit on canopy temperature. Maes and Steppe (2012) have shown that the effect of radiation on canopy temperature is higher on canopies with high stomatal conductance (T_{wet}) compared to canopies with low stomatal conductance (T_{dry}). Since in this study solar radiation measured at the different seasons ranged from 831 to 1012 w/m^2 , CWSI was significantly affected by it, thus explaining the major contribution of solar radiation on the four season's regression model. Agam et al., (2013a, 2013b) have shown a major effect of clouds on CWSI calculation. However, more study on the effect of solar radiation on CWSI calculations should be invested under clear sky conditions. Meanwhile, our results suggest that in multi-season calibration CWSI- Ψ_{stem} models, radiation should be considered. The contribution of seasonal cumulative variables, together with the effect of solar radiation, on T_{wet} was not quantified by the model based solely on CWSI, and thus elucidates the higher proportion of the variation of Ψ_{stem} explained by the four-parameter model. Spatial factors such as CWSI are expected to play a substantial role in accurately forecasting Ψ_{stem} in smaller-scale models that offer detailed spatial representation, such as MZ and MC. However, their contribution is likely to be less pronounced in models predicting Ψ_{stem} at a larger scale, such as the vineyard scale. Nevertheless, CWSI, which was the only parameter that represented the spatial variability of the canopy water status within the vineyard, contributed most to the prediction of the measured Ψ_{stem} at all scales (Fig. 4).

Conclusions

The results presented in this study demonstrate the complexity in using thermal imagery for water status estimation in vineyards and its consequential use in irrigation decision-making. First, CWSI- Ψ_{stem} relationships were found to be affected by scale size that should be accounted for when establishing thermal-based water status assessments in vineyards. The accuracy of the thermal-based model increased with increasing size of scale. Second, the CWSI- Ψ_{stem} relationships were not stable over time. Model robustness required a minimum of two training seasons and benefited from incorporation of additional meteorological parameters, especially radiation and accumulative ET_0 . Despite CWSI limitations, it was shown for the first time that at both the vineyard (2.5 ha) and MC (0.09 ha) scales, the thermal-based model predicted Ψ_{stem} better than best management water status monitoring practice, i.e., direct measurements of a few representative vines. Further, the study's results suggest that Ψ_{stem} predicted by CWSI (based on UAV thermal imagery) could benefit both uniform and precision irrigation. Future studies should evaluate precision irrigation in on-farm experimentation to explore its actual effect on yield parameters and on irrigation water use efficiency. Utilizing the insights from the spatial and temporal aspects explored in this study relating to CWSI- Ψ_{stem} relationships may pave the way for expanding the utilization of thermal imagery in irrigation decision support systems.

Appendix

See Table 6 and Fig. 7.

Table 6 Model accuracy attributes with different number of seasons required for calibrating (cal) and testing Ψ_{stem} values (test)

Model	3p1	2p2	2p1	1p2	1p1	1p3
No. of Combinations	4	6	12	12	12	4
Cal (n)	260–380	140–300	140–300	60–180	60–180	60–180
Test (n)	60–180	140–300	60–180	140–300	60–180	260–380
Mean RMSE	0.1336	0.1426	0.1411	0.1601	0.1580	0.1611
Std RMSE	0.0148	0.0131	0.0156	0.0171	0.0215	0.0156
Mean R^2	0.6029	0.5867	0.5543	0.4304	0.4407	0.4888
Std R^2	0.0881	0.0926	0.1067	0.0639	0.1421	0.0890

The calibration/test ratio is shown in bold. e.g., 3p1 – three seasons used to predict single season of Ψ_{stem} values with four different combinations

Each season had a different number of campaign dates (Table 3), causing them to have different repetition number for calibration and test.

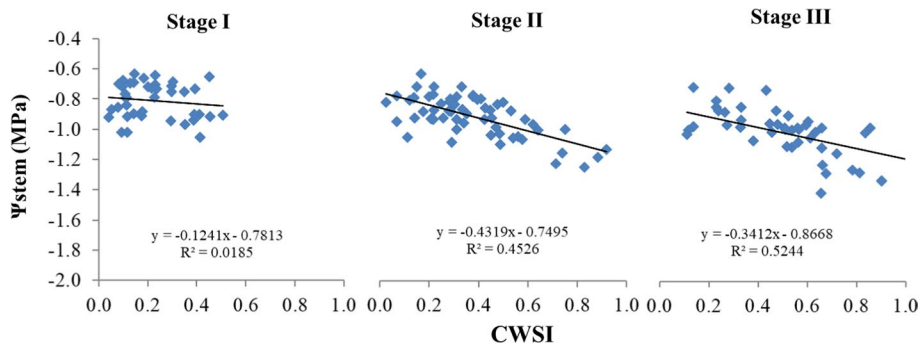


Fig. 7 CWSI and Ψ_{stem} correlations in studied vineyard (in Mevo-Betar) at three phenological growth stages (Coombe & McCarthy, 2000) in 2018. Stage I – 23/5 – 6/6, stage II – 20/6 – 18/7, stage III – 31/7 – 29/8. Each dot represents management cell (n=20 for each measurement day)

Acknowledgements This research was a part of the “Eugene Kendel” Project for the Development of Precision Drip Irrigation funded via the Ministry of Agriculture and Rural Development in Israel (Grant No. 20-12-0030). The project also received funding from the European Union’s Horizon 2020 research and innovation programme under Project SHui, grant agreement No 773903. The authors wish to thank ‘Carmel Winery’ for their contribution for the study. We thank Avi Yehuda and Dror Dotan from the agricultural department of ‘Carmel Winery’. We thank Ben Hazut, Matan Golomb, Doron Kleiman and Gal Mat for their accurate field measurements.

Funding Open access funding provided by Hebrew University of Jerusalem. Eugene Kendel” Project for the Development of Precision Drip Irrigation funded via the Ministry of Agriculture and Rural Development in Israel, 20-12-0030, Yafit Cohen, European Union’s Horizon 2020

Data availability The data that support the findings of this study are available from the corresponding author, [I.B], upon reasonable request.

Open Access This article is licensed under a Creative Commons Attribution 4.0 International License, which permits use, sharing, adaptation, distribution and reproduction in any medium or format, as long as you give appropriate credit to the original author(s) and the source, provide a link to the Creative Commons licence, and indicate if changes were made. The images or other third party material in this article are included in the article's Creative Commons licence, unless indicated otherwise in a credit line to the material. If material is not included in the article's Creative Commons licence and your intended use is not permitted by statutory regulation or exceeds the permitted use, you will need to obtain permission directly from the copyright holder. To view a copy of this licence, visit <http://creativecommons.org/licenses/by/4.0/>.

References


- Acevedo-Opazo, C., Ortega-farias, S., & Fuentes, S. (2010). Effects of grapevine (*Vitis vinifera* L.) water status on water consumption, vegetative growth and grape quality: An irrigation scheduling application to achieve regulated deficit irrigation. *Agricultural Water Management*, 97(7), 956–964. <https://doi.org/10.1016/j.agwat.2010.01.025>
- Agam, N., Cohen, Y., Berni, J. A. J., Alchanatis, V., Kool, D., Dag, A., Yermiyahu, U., & Ben-Gal, A. (2013a). An insight to the performance of crop water stress index for olive trees. *Agricultural Water Management*, 118, 79–86. <https://doi.org/10.1016/j.agwat.2012.12.004>
- Agam, N., Cohen, Y., Alchanatis, V., & Ben-Gal, A. (2013b). How sensitive is the CWSI to changes in solar radiation? *International Journal of Remote Sensing*, 34(17), 6109–6120. <https://doi.org/10.1080/01431161.2013.793873>
- Alchanatis, V., Cohen, S., Moller, M., Sprinstin, M., Meron, M., Tsipris, J., Saranga, Y., & Sela, E. (2010). Evaluation of different approaches for estimating and mapping crop water status in cotton with thermal imaging. *Precision Agriculture*, 11(1), 27–41. <https://doi.org/10.1007/s11119-009-9111-7>
- Alchanatis, V., & Shkolnik, E. (2023). *Controllable dripper valve and system thereof*. WIPO.
- Allen, R. G., Pruitt, W. O., Wright, J. L., Howell, T. A., Ventura, F., Snyder, R., Itenfisu, D., Steduto, P., Berengena, J., Yrisarry, J. B., Smith, M., Pereira, L. S., Raes, D., Perrier, A., Alves, I., Walter, I., & Elliott, R. (2006). A recommendation on standardized surface resistance for hourly calculation of reference ETo by the FAO56 Penman–Monteith method. *Agricultural Water Management*, 81(1–2), 1–22. <https://doi.org/10.1016/j.agwat.2005.03.007>
- Arno, J., Uribeetxebarria, A., Llorens, J., Escola, A., Rosell-polo, J. R., Gregorio, E., & Martinez-Casasnovas, J. A. (2023). Drip irrigation soil-adapted sector design and optimal location of moisture sensors: A case study in a vineyard plot. *Agronomy*. <https://doi.org/10.3390/agronomy13092369>
- Atkinson, P. M., Sargent, I. M., Foody, G. M., & Williams, J. (2007). Exploring the geostatistical method for estimating the signal-to-noise ratio of images. *Photogrammetric Engineering and Remote Sensing*, 73(7), 841–850. <https://doi.org/10.14358/PERS.73.7.841>
- Bahat, I., Netzer, Y., Ben-Gal, A., Grünzweig, J. M., Peeters, A., & Cohen, Y. (2019). Comparison of water potential and yield parameters under uniform and variable rate drip irrigation in a cabernet sauvignon vineyard. *Precision Agriculture 2019 - Papers Presented at the 12th European Conference on Precision Agriculture, ECPA 2019*. https://doi.org/10.3920/978-90-8686-888-9_14
- Bahat, I., Netzer, Y., Grünzweig, J. M., Alchanatis, V., Peeters, A., Goldshtein, E., Ohana-Levi, N., Ben-Gal, A., & Cohen, Y. (2021). In-season interactions between vine vigor, water status and wine quality in terrain-based management-zones in a ‘cabernet sauvignon’ vineyard. *Remote Sensing*, 13(9), 1636. <https://doi.org/10.3390/rs13091636>
- Baluja, J., Diago, M. P., Balda, P., Zorer, R., Meggio, F., Morales, F., & Tardaguila, J. (2012). Assessment of vineyard water status variability by thermal and multispectral imagery using an unmanned aerial vehicle (UAV). *Irrigation Science*, 30(6), 511–522. <https://doi.org/10.1007/s00271-012-0382-9>
- Bellvert, J., Marsal, J., Girona, J., Gonzalez-Dugo, V., Fereres, E., Ustin, S. L., & Zarco-Tejada, P. J. (2016a). Airborne thermal imagery to detect the seasonal evolution of crop water status in peach, nectarine and saturn peach orchards. *Remote Sensing*, 8(1), 1–17. <https://doi.org/10.3390/rs8010039>
- Bellvert, J., Marsal, J., Girona, J., & Zarco-Tejada, P. J. (2014a). Seasonal evolution of crop water stress index in grapevine varieties determined with high-resolution remote sensing thermal imagery. *Irrigation Science*, 33(2), 81–93. <https://doi.org/10.1007/s00271-014-0456-y>
- Bellvert, J., Zarco-Tejada, P. J., Girona, J., & Fereres, E. (2014b). Mapping crop water stress index in a ‘Pinot-noir’ vineyard: Comparing ground measurements with thermal remote sensing imagery from an unmanned aerial vehicle. *Precision Agriculture*, 15(4), 361–376. <https://doi.org/10.1007/s11119-013-9334-5>

- Bellvert, J., Zarco-Tejada, P. J., Marsal, J., Girona, J., González-Dugo, V., & Fereres, E. (2016b). Vineyard irrigation scheduling based on airborne thermal imagery and water potential thresholds. *Australian Journal of Grape and Wine Research*, 22(2), 307–315. <https://doi.org/10.1111/ajgw.12173>
- Ben-Gal, A., Cohen, Y., Peeters, A., Naor, A., Nezer, Y., Ohana-Levi, N., Bahat, I., Katz, L., Shaked, B., Linker, R., Yulzary, S., & Alchanatis, V. (2022). Precision drip irrigation for horticulture. *Acta Horticulturae*, 1335, 267–274. <https://doi.org/10.17660/ActaHortic.2022.1335.32>
- Berrar, D. (2018). Cross-validation. *Encyclopedia of Bioinformatics and Computational Biology: ABC of Bioinformatics*, 1–3, 542–545. <https://doi.org/10.1016/B978-0-12-809633-8.20349-X>
- Bian, J., Zhang, Z., Chen, J., Chen, H., Cui, C., Li, X., Chen, S., & Fu, Q. (2019). Simplified evaluation of cotton water stress using high resolution unmanned aerial vehicle thermal imagery. *Remote Sensing*, 11(3), 267. <https://doi.org/10.3390/rs11030267>
- Boyer, J. S. (1995). *Measuring water status of plants* (pp. 13–48). Academic Press.
- Budescu, D. V. (1993). Dominance analysis: A new approach to the problem of relative importance of predictors in multiple regression. *Psychological Bulletin*, 114(3), 542–551. <https://doi.org/10.1037/0033-2909.114.3.542>
- Cai, L., & Zhu, Y. (2015). The challenges of data quality and data quality assessment in the big data era. *Data Science Journal*, 14, 1–10. <https://doi.org/10.5334/dsj-2015-002>
- Choné, X., van Leeuwen, C., Dubourdieu, D., & Guadilleare, J. P. (2001). Stem water potential is a sensitive indicator of grapevine water status. *Annals of Botany*, 87, 477–483. <https://doi.org/10.1006/anbo.2000.1361>
- Cohen, Y., & Alchanatis, V. (2018). Spectral and spatial methods for hyperspectral and thermal image-analysis to estimate biophysical and biochemical properties of agricultural crops. In S. T. Prasad, G. L. John, & H. Alfredo (Eds.), *Biophysical and biochemical characterization and plant species studies*. CRC Press.
- Cohen, Y., Alchanatis, V., Meron, M., Saranga, Y., & Tsipris, J. (2005). Estimation of leaf water potential by thermal imagery and spatial analysis. *Journal of Experimental Botany*, 56(417), 1843–1852. <https://doi.org/10.1093/jxb/eri174>
- Cohen, Y., Alchanatis, V., Saranga, Y., Rosenberg, O., Sela, E., & Bosak, A. (2017). Mapping water status based on aerial thermal imagery: Comparison of methodologies for upscaling from a single leaf to commercial fields. *Precision Agriculture*, 18(5), 801–822. <https://doi.org/10.1007/s11119-016-9484-3>
- Cohen, Y., Alchanatis, V., Sela, E., Saranga, Y., Cohen, S., Meron, M., Bosak, A., Tsipris, J., Ostrovsky, V., Orolov, V., Levi, A., & Brikman, R. (2015). Crop water status estimation using thermography: Multi-year model development using ground-based thermal images. *Precision Agriculture*, 16(3), 311–329. <https://doi.org/10.1007/s11119-014-9378-1>
- Cohen, Y., Vellidis, G., Campillo, C., Laikos, V., Graff, N., Saranga, Y., Snider, J. L., Casadesus, J., Milan, S., & Prieto del Haner, M. (2021). Applications of sensing to precision irrigation. In R. Kerry & A. Escolà (Eds.), *Sensing approaches for precision agriculture*. Springer.
- Coombe, B. G., & McCarthy, M. G. (2000). Dynamics of grape berry growth and physiology of ripening. *Australian Journal of Grape and Wine Research*, 6(2), 131–135. <https://doi.org/10.1111/j.1755-0238.2000.tb00171.x>
- Fuentes, S., de Bei, R., Pech, J., & Tyerman, S. (2012). Computational water stress indices obtained from thermal image analysis of grapevine canopies. *Irrigation Science*, 30(6), 523–536. <https://doi.org/10.1007/s00271-012-0375-8>
- Ghosh, D., & Kaabouch, N. (2016). A survey on image mosaicing techniques. *Journal of Visual Communication and Image Representation*, 34, 1–11. <https://doi.org/10.1016/j.jvcir.2015.10.014>
- Gonzalez-Dugo, V., & Zarco-Tejada, P. J. (2022). Assessing the impact of measurement errors in the calculation of CWSI for characterizing the water status of several crop species. *Irrigation Science*. <https://doi.org/10.1007/s00271-022-00819-6>
- Grant, O. M., Tronina, L., Jones, H. G., & Chaves, M. M. (2007). Exploring thermal imaging variables for the detection of stress responses in grapevine under different irrigation regimes. *Journal of Experimental Botany*, 58(4), 815–825. <https://doi.org/10.1093/jxb/eri153>
- Gutiérrez, S., Diago, M. P., Fernández-Navales, J., & Tardaguila, J. (2018). Vineyard water status assessment using on-the-go thermal imaging and machine learning. *PLoS ONE*, 13(2), e0192037. <https://doi.org/10.1371/journal.pone.0192037>
- Helman, D., Bahat, I., Netzer, Y., Ben-Gal, A., Alchanatis, V., Peeters, A., & Cohen, Y. (2018). Using time series of high-resolution planet-satellite images to monitor grapevine stem water potential in commercial vineyards. *Remote Sensing*, 10(10), 1–22. <https://doi.org/10.3390/rs10101615>
- Herrera, J. C., Calderan, A., Gambetta, G. A., Peterlunger, E., Forneck, A., Sivilotti, P., Cochard, H., & Hochberg, U. (2022). Stomatal responses in grapevine become increasingly more tolerant to low

- water potentials throughout the growing season. *Plant Journal*, 109(4), 804–815. <https://doi.org/10.1111/tpj.15591>
- Hijmans, R. J., Etten, J. van, Sumner, M., Cheng, J., Bevan, A., Bevan, R., Busetto, L., Canty, M., Forrest, D., Ghosh, A., Golicher, D., Gray, J., & Greenberg, J. A. (2020). Package “raster.” *Cran*, 1–249. <https://cran.r-project.org/web/packages/raster/raster.pdf>
- Idso, S. B., Jackson, R. D., Pinter, P. J., Reginato, R. J., & Hatfield, J. L. (1981). Normalizing the stress-degree-day parameter for environmental variability. *Agricultural Meteorology*. [https://doi.org/10.1016/0002-1571\(81\)90032-7](https://doi.org/10.1016/0002-1571(81)90032-7)
- Jackson, R. D., Idso, S. B., Reginato, R. J., & Pinter, P. J. (1981). Canopy temperature as a crop water stress indicator. *Water Resources Research*, 17(4), 1133–1138. <https://doi.org/10.1029/WR017i004p01133>
- Jones, G. V., White, M. A., Cooper, O. R., & Storchmann, K. (2005). Climate change and global wine quality. *Climatic Change*, 73(3), 319–343. <https://doi.org/10.1007/s10584-005-4704-2>
- Jones, H. G. (1999). Use of infrared thermometry for estimation of stomatal conductance as a possible aid to irrigation scheduling. *Agricultural and Forest Meteorology*, 95(3), 139–149. [https://doi.org/10.1016/S0168-1923\(99\)00030-1](https://doi.org/10.1016/S0168-1923(99)00030-1)
- Jones, H. G., & Sirault, X. R. R. (2014). Scaling of thermal images at different spatial resolution: The mixed pixel problem. *Agronomy*, 4(3), 380–396. <https://doi.org/10.3390/agronomy4030380>
- Kamilaris, A., Kartakoullis, A., & Prenafeta-Boldú, F. X. (2017). A review on the practice of big data analysis in agriculture. *Computers and Electronics in Agriculture*, 143, 23–37. <https://doi.org/10.1016/j.compag.2017.09.037>
- Katz, L., Ben-Gal, A., Litaor, M. I., Naor, A., Peres, M., Bahat, I., Netzer, Y., Peeters, A., Alchanatis, V., & Cohen, Y. (2022). Spatiotemporal normalized ratio methodology to evaluate the impact of field-scale variable rate application. *Precision Agriculture*, 23, 1125–1152. <https://doi.org/10.1007/s11119-022-09877-4>
- Maes, W., & Steppe, K. (2012). Estimating evapotranspiration and drought stress with ground-based thermal remote sensing in agriculture: A review. *Journal of Experimental Botany*, 63(13), 4671–4712. <https://doi.org/10.1093/jxb/err313>
- Matese, A., Baraldi, R., Berton, A., Cesaraccio, C., Di Gennaro, S. F., Duce, P., Facini, O., Mameli, M. G., Piga, A., & Zaldei, A. (2018). Estimation of water stress in grapevines using proximal and remote sensing methods. *Remote Sensing*, 10(1), 1–16. <https://doi.org/10.3390/rs10010114>
- Matese, A., & Di Gennaro, S. F. (2018). Practical applications of a multisensor UAV platform based on multispectral, thermal and RGB high resolution images in precision viticulture. *Agriculture (switzerland)*. <https://doi.org/10.3390/agriculture8070116>
- Meron, M., Tsipris, J., Orlov, V., Alchanatis, V., & Cohen, Y. (2010). Crop water stress mapping for site-specific irrigation by thermal imagery and artificial reference surfaces. *Precision Agriculture*, 11(2), 148–162. <https://doi.org/10.1007/s11119-009-9153-x>
- Möller, M., Alchanatis, V., Cohen, Y., Meron, M., Tsipris, J., Naor, A., Ostrovsky, V., Sprintsin, M., & Cohen, S. (2007). Use of thermal and visible imagery for estimating crop water status of irrigated grapevine. *Journal of Experimental Botany*, 58(4), 827–838. <https://doi.org/10.1093/jxb/erl115>
- Munitz, S., Schwartz, A., & Netzer, Y. (2019). Water consumption, crop coefficient and leaf area relations of a *Vitis vinifera* cv. “Cabernet Sauvignon” vineyard. *Agricultural Water Management*, 219, 86–94. <https://doi.org/10.1016/j.agwat.2019.03.051>
- Naor, A. (1998). Relations between leaf and stem water potentials and stomatal conductance in three field-grown woody species. In *Journal of Horticultural Science & Biotechnology*, 73(4), 431–436.
- Ndlovu, H. S., Odindi, J., Sibanda, M., Mutanga, O., Clulow, A., Chimonyo, V. G. P., & Mabhaudhi, T. (2021). A comparative estimation of maize leaf water content using machine learning techniques and unmanned aerial vehicle (UAV)-based proximal and remotely sensed data. *Remote Sensing*, 13(20), 4091.
- Netzer, Y., Munitz, S., Shtein, I., & Schwartz, A. (2019). Structural memory in grapevines : Early season water availability affects late season drought stress severity. *European Journal of Agronomy*, 105, 96–103. <https://doi.org/10.1016/j.eja.2019.02.008>
- Netzer, Y., Yao, C., Shenker, M., Bravdo, B. A., & Schwartz, A. (2009). Water use and the development of seasonal crop coefficients for superior seedless grapevines trained to an open-gable trellis system. *Irrigation Science*, 27(2), 109–120. <https://doi.org/10.1007/s00271-008-0124-1>
- Oger, B., Vismara, P., & Tisseyre, B. (2021). Combining target sampling with within field route - optimization to optimise on field yield estimation in viticulture. *Precision Agriculture*, 22(2), 432–451. <https://doi.org/10.1007/s11119-020-09744-0>
- Ohana-levi, N., Cohen, Y., Munitz, S., Michaelovsky, R., Ferman, D., Hagag, N., Getz, Y., & Netzer, Y. (2024). The response of yield, number of clusters, and cluster weight to meteorological factors and

- irrigation practices in grapevines : A multi-experiment study. *Scientia Horticulturae*. <https://doi.org/10.1016/j.scienta.2023.112761>
- Ohana-Levi, N., Derumigny, A., Peeters, A., Ben-Gal, A., Bahat, I., Katz, L., Netzer, Y., Naor, A., & Cohen, Y. (2021). A multifunctional matching algorithm for sample design in agricultural plots. *Computers and Electronics in Agriculture*, 187, 106262. <https://doi.org/10.1016/j.compag.2021.106262>
- Ohana-Levi, N., Mintz, D. F., Hagag, N., Stern, Y., Munitz, S., Friedman-Levi, Y., Shacham, N., Grünzweig, J. M., & Netzer, Y. (2022). Grapevine responses to site-specific spatiotemporal factors in a mediterranean climate. *Agricultural Water Management*. <https://doi.org/10.1016/j.agwat.2021.107226>
- Ohana-Levi, N., Munitz, S., Ben-Gal, A., Schwartz, A., Peeters, A., & Netzer, Y. (2020). Multiseasonal grapevine water consumption – drivers and forecasting. *Agricultural and Forest Meteorology*, 280, 107796. <https://doi.org/10.1016/j.agrformet.2019.107796>
- Ortuani, B., Facchi, A., Mayer, A., Bianchi, D., & Brancadoro, L. (2019). Assessing the effectiveness of variable-rate drip irrigation on water use efficiency in a vineyard in Northern Italy. *Water*, 11(10), 1964. <https://doi.org/10.3390/w11101964>
- Pou, A., Diago, M. P., Medrano, H., Baluja, J., & Tardaguila, J. (2014). Validation of thermal indices for water status identification in grapevine. *Agricultural Water Management*, 134, 60–72. <https://doi.org/10.1016/j.agwat.2013.11.010>
- R Core Team. (2019). R: A language and environment for statistical computing. Retrieved September 1, 2020.
- Romero, M., Luo, Y., Su, B., & Fuentes, S. (2018). Vineyard water status estimation using multispectral imagery from an UAV platform and machine learning algorithms for irrigation scheduling management. *Computers and Electronics in Agriculture*, 147, 109–117. <https://doi.org/10.1016/j.compag.2018.02.013>
- Rud, R., Cohen, Y., Alchanatis, V., Levi, A., Brikman, R., Shenderey, C., Heuer, B., Markovitch, T., Dar, Z., Rosen, C., Mulla, D., & Nigon, T. (2014). Crop water stress index derived from multi-year ground and aerial thermal images as an indicator of potato water status. *Precision Agriculture*, 15(3), 273–289. <https://doi.org/10.1007/s11119-014-9351-z>
- Sanchez, L. A., Sams, B., Alsina, M. M., Hinds, N., Klein, L. J., & Dokoozlian, N. (2017). Improving vineyard water use efficiency and yield with variable rate irrigation in California. *Advances in Animal Biosciences*, 8(02), 574–577. <https://doi.org/10.1017/S2040470017000772>
- Santesteban, L. G., Di Gennaro, S. F., Herrero-Langreo, A., Miranda, C., Royo, J. B., & Matese, A. (2017). High-resolution UAV-based thermal imaging to estimate the instantaneous and seasonal variability of plant water status within a vineyard. *Agricultural Water Management*, 183, 49–59. <https://doi.org/10.1016/j.agwat.2016.08.026>
- Santesteban, L. G., Miranda, C., Marín, D., Sesma, B., Intrigliolo, D. S., Mirás-Avalos, J. M., Escalona, J. M., Montoro, A., de Herralde, F., Baeza, P., Romero, P., Yuste, J., Uriarte, D., Martínez-Gascuña, J., Cancela, J. J., Pinillos, V., Loidi, M., Urrestarazu, J., & Royo, J. B. (2019). Discrimination ability of leaf and stem water potential at different times of the day through a meta-analysis in grapevine (*Vitis vinifera* L.). *Agricultural Water Management*, 221, 202–210. <https://doi.org/10.1016/j.agwat.2019.04.020>
- Sepúlveda-Reyes, D., Ingram, B., Bardeen, M., Zúñiga, M., Ortega-Farías, S., & Poblete-Echeverría, C. (2016). Selecting canopy zones and thresholding approaches to assess grapevine water status by using aerial and ground-based thermal imaging. *Remote Sensing*. <https://doi.org/10.3390/rs8100822>
- Shaked, B. (2023). Development of a model for estimating the effective transmission distance of wireless communication in a cotton field. [Master's thesis, Technion—Israel Institute of Technology].
- Tisseyre, B., Leroux, C., Pichon, L., Geraudie, V., & Sari, T. (2018). How to define the optimal grid size to map high resolution spatial data? *Precision Agriculture*, 19(5), 957–971. <https://doi.org/10.1007/s11119-018-9566-5>
- Van Leeuwen, C., Tregoat, O., Choné, X., Bois, B., Pernet, D., & Gaudillere, J. P. (2009). Vine water status is a key factor in grape ripening and vintage quality for red Bordeaux wine. How can it be assessed for vineyard management purposes? *OENO One*, 43(3), 121–134. <https://doi.org/10.20870/OENO-ONE.2009.43.3.798>

Authors and Affiliations

Idan Bahat^{1,2}  · **Yishai Netzer^{3,4}** · **José M. Grünzweig²** · **Amos Naor⁵** · **Victor Alchanatis¹** · **Alon Ben-Gal⁶** · **Ohali'av Keisar¹** · **Guy Lidor¹** · **Yafit Cohen¹**

✉ Idan Bahat
idan.bahat@mail.huji.ac.il

¹ Institute of Agricultural Engineering, Agricultural Research Organization (Volcani Center), P.O. Box 15159, 7505101 Rishon LeZion, Israel

² The Robert H. Smith Faculty of Agriculture, Food & Environment, The Robert H. Smith Institute of Plant Sciences and Genetics in Agriculture, The Hebrew University of Jerusalem, 76100 Rehovot, Israel

³ Department of Agriculture and Oenology, Eastern R&D Center, Ariel, Israel

⁴ Department of Chemical Engineering, Ariel University, 40700 Ariel, Israel

⁵ Department of Precision Agriculture, MIGAL Galilee Research Institute, P.O.B. 831, 11016 Kiryat Shmona, Israel

⁶ Department of Soil, Water and Environmental Sciences, Agricultural Research Organization, Gilat Research Center, Mobile Post Negev 2, 85280 Gilat, Israel